J. A. Duffie

J. W. Mitchell

Solar Energy Laboratory,
University of Wisconsin-Madison,
Madison, Wis. 53706

f-Chart: Predictions and Measurements

1 Introduction

The *f*-chart method for predicting the annual performance of solar heating systems has come into widespread use since its publication in 1976 and 1977. For several years, only a limited data base of measured performance of systems has been available allowing general comparisons to be made of predicted and measured performance. The data base is now improved; the purpose of this paper is to summarize the comparisons and outline reasons why measured performance data do or do not agree with predictions.

The design method is based on correlation of the results of a large number of detailed, hour-by-hour simulations of solar heating systems. *f*-chart annual performance estimates have been checked against detailed simulations for many U.S. locations, with agreement generally in the range of ±3 percent and within ±11 percent in the worst case (Seattle). Simulations have been compared with detailed measurements on real systems for periods on the order of days, again with satisfactory results. In this paper we compare the annual performance results of *f*-chart with annual or seasonal measured performance, the third in a hierachy of steps in the validation of the method and the simulations on which it is based.

2 The *f*-Chart Method

The *f*-chart correlations [1–3] were developed for predicting the annual performance of solar space heating systems of two standard configurations. The standard liquid system configuration is shown in Fig. 1. The range of design parameters used in developing the correlation is given in Table 1. Several assumptions were made, most of which tend to lead to conservative predictions of performance. For example, a fully mixed storage tank was assumed, and the method of processing solar radiation data led to conservative estimates of solar contribution. On the other hand, it was assumed that controls were such that energy in the storage tank could be delivered to the load as long as its temperature was above the room temperature of 20°C. This relatively low temperature may lead to overestimates of collected energy. Auxiliary energy for space heating is added in parallel with solar; i.e., solar was assumed to supply as much as it could, and auxiliary provided the balance of the needed energy.

Contributed by the Solar Energy Division for publication in the JOURNAL OF SOLAR ENERGY ENGINEERING. Manuscript received by the Solar Energy Division March 26, 1982.

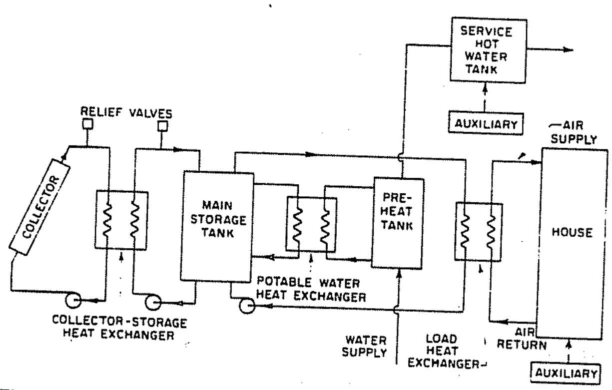

Fig. 1 Schematic of the standard *f*-chart system configuration for space heating using a liquid storage tank

Table 1 Ranges of design parameters used in developing the *f*-charts for liquid systems, and ranges of parameters covered by correction factors [1, 4]

$0.6 \le (\tau\alpha)_n$	≤ 0.9
$5 \le F_R A$	$\le 120 \text{m}^2$
$2.1 \le U_L$	$\le 8.3 \text{ W/m}^2\text{C}$
$30 \le \beta$	≤ 80 deg
$83 \le (UA)_h$	≤ 667 W/C

Storage capacity

$$37.5 \le \text{Store Cap} \le 300\ l/\text{m}^2$$

Load heat exchanger

$$0.5 \le \left(\frac{\epsilon_l C_{\min}}{(UA)_h}\right) \le 50$$

The standard air system configuration is shown in Fig. 2, and the range of design parameters is indicated Table 2. For these systems, stratification in the pebble bed storage unit was accounted for, and auxiliary was again assumed to be added in parallel.

An *f*-chart correlation was also developed for hot water systems. In this case, the *f*-chart itself (and the equation describing the correlation) is the same as for liquid space heating systems, but the dimensionless variable X was redefined to include the supply water temperature and the delivery water temperature. The latter was constrained to the

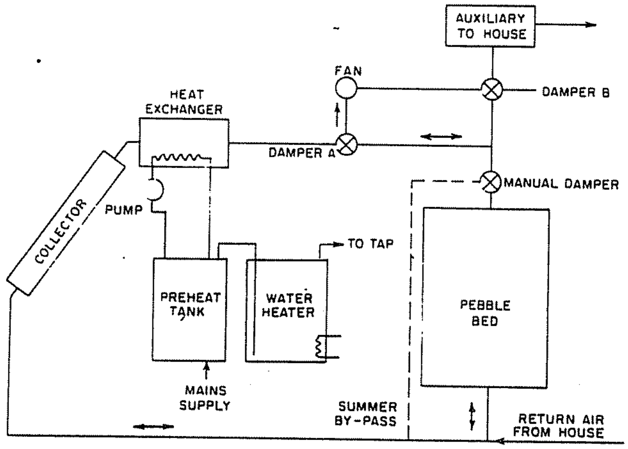

Fig. 2 Schematic of the standard *f*-chart air system configuration for space heating using pebble bed storage

Table 2 Ranges of design parameters used in developing the *f*-chart for air systems, and ranges of parameters covered by correction factors [2, 4]

$0.6 \le (\tau\alpha)_n$	≤ 0.9
$5 \le F_R A$	$\le 120\text{m}^2$
$2.1 \le U_L$	$\le 8.3\ \text{W/m}^2\text{C}$
$30 \le \beta$	≤ 90 deg
$83 \le (UA)_h$	≤ 667 W/C

Storage size

$0.125 \le$ store volume $\le 1.00\ \text{m}^3/\text{m}^2$

Air flow rate in collector

$5 \le$ volumetric flow $\le 20\ l/\text{m}^2\text{s}$

range of 40 to 60°C. A two-tank system was assumed, as shown in Fig. 3. Standard losses were assumed to occur from a well-insulated preheat tank, and losses from the auxiliary tank should be included as part of the heating loads on the system.

The *f*-chart correlations for monthly performance apply over limited ranges of the dimensionless variables X and Y. X and Y can be written

$$X = F_R U_L \frac{F_R'}{F_R} (T_{\text{ref}} - \bar{T}_a) \Delta t A_c / L$$

$$Y = F_R (\tau\alpha)_n \frac{(\tau\alpha)}{(\tau\alpha_n)} \frac{F_R'}{F_R} \bar{H}_T N A_c / L$$

The parameters include $F_R(\tau\alpha)_n$ and $F_R U_L$, the intercept and slope of the collector test curves. These are modified by a set of factors, including $(\tau\alpha)/(\tau\alpha)_n$ and F_R'/F_R. They may also be modified to account for duct and pipe losses (5), if these are to ambient and are in fact losses. In addition, correction factors for the sizes of the load heat exchanger and storage tank (for liquid systems) and for the air flow rate and pebble bed store size (for air systems) were developed for limited ranges of these variables, as indicated in Tables 1 and 2.

While the *f*-charts yield a month-by-month estimates of the solar contribution to heating and hot water loads, they are intended to be a means for arriving at annual or seasonal solar contributions. As stated in [1], the *f*-chart "is not intended to provide an accurate estimate of systems performance for any particular month, but rather for the year." All comparisons in this paper are of predicted and measured performance for at least the major part of the heating season.

There are several possible definitions of f, the monthly (or F, the annual) contributions of solar energy, as noted by Buckles and Klein [6]. In their nomenclature, the two which should be distinguished are

$$f_2 = 1 - \text{auxiliary/load}$$
$$f_3 = 1 - \text{auxiliary with solar/auxiliary without solar}$$

In the *f*-chart method, the load is the energy needed to heat the building and/or water plus (for two-tank water heaters) losses from the auxiliary tank. Thus, it is the energy that would be supplied if there were no solar energy system. As long as the presence of the solar energy system does not affect the loads, f_2 and f_3 are the same. If, however, the solar energy system affects the load, they are not identical. This can happen, for example, if a solar heating system keeps the building temperature higher within a control band than does a conventional system, or if during mild weather auxiliary energy is turned off and occupants settle for lower building or water temperatures. The solar fractions reported here are values of f_2.

(It is useful to distinguish between the *f*-chart method and FCHART 3, an interactive program that is convenient for doing the necessary calculations. There is also an FCHART 4 program that uses the *f*-chart correlation for air systems, but uses a different method (utilizability) for liquid and DHW systems. The resuls of calculations of liquid and DHW systems done with FCHART 4 will be close to but not identical with those done with FCHART 3. All of the results included in this paper are for *f*-chart predictions, with calculations made by hand or with FCHART 3.)

3 Data Sources and Comparisons

Differences between predicted and measured performance, i.e., between F_P and F_M, can arise for several reasons. First, the system may not be close in configuration, parameter ranges, or control strategy to one of the standard systems. Second, there may be defects in the details of design or installation of the system. Third, reliable measurements of solar radiation and system performance are not easy to make, an-

Nomenclature

A_c = collector area
$C_{\min}$ = minimum capacitance rate
F_M = measured fraction of load met by solar energy
F_P = predicted fraction of load met by solar energy
F_R = collector heat removal factor
F_R'/F_R = collector heat exchanger correction factor
$\bar{H}_T$ = monthly average daily radiation on collector, per unit area
L = monthly heating load
N = number of days in month
$\bar{T}_a$ = monthly average ambient temperature
T_{ref} = an (empirical) reference temperature, 100°C (212°F)
Δt = number of time units in a month (seconds if U_L is in watts, hours is in hours)
U_L = collector overall loss coefficient
$(UA)_h$ = loss coefficient-area product of building
β = slope of collector
ϵ_l = effectiveness of load heat exchanger
$(\tau\alpha)$ = transmittance-absorptance product of collector
$(\tau\alpha)$ = transmittance-absorptance product at normal incidence

Table 3

Year	F_P	F_M
1959–60	0.56	0.48
1960–61	0.62	0.57

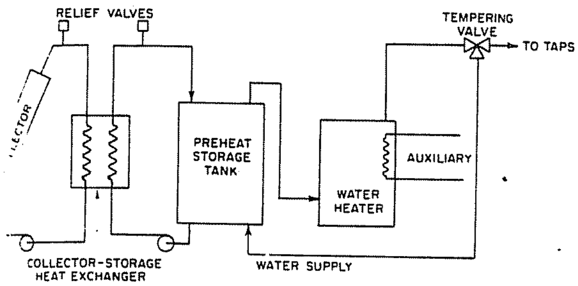

Fig. 3 Schematic of the standard f-chart system configuration for water heating only. Collector fluid may be either air or water

measurement errors in either may contribute to apparent differences. Fourth, f-chart calculations may be in error, as it is not always clear from the reported calculated performance exactly how the f-chart analyses have been done (for example, how losses for storage tanks, ducts, and piping have been accounted for, or whether $F_R\ (\tau\alpha)_n$ and $F_R U_L$ values used are from *in situ* measurements or laboratory tests). Fifth, there is the basic question addressed in this paper: does f-chart represent the long-term performance, for systems that show differences not attributed to any of the first four reasons?

The original f-chart paper [1] included a comparison of results for MIT House IV operation for each of two years. These were the only data available in 1976, and are shown in Table 3. The system configuration was not identical to that of Fig. 1, in that the system used drain-back freeze protection. It was a system development experiment, and Engebretson [7] stated that performance could have been expected to improve with further operating experience with the system. The initial comparison were encouraging.

A few other comparisons have been made. Fanney [8] compares measured with predicted results of solar water heaters in NBS laboratories. The Solar Energy Applications Laboratory of Colorado State University has made careful measurements of a year's performance of each of several types of air and liquid systems, and comparisons for three of these systems are included [9, 10]. Faiman et al. [11] have monitored a year's operation of a water heating system at a Negev kibbutz, and compared the measured with the predicted output. The results of these authors are included in this summary.

The National Solar Data Network (NSDN) has provided measured performance data on a wide variety of systems in all parts of the United States, and their reports include the predicted solar contribution using f-chart. The systems for which we show comparisons of NSDN data are systems that are reasonably close (but not in all respects identical) in configuration to the standard f-chart configurations; these are systems for which f-chart might legitimately be used for design. Some of the data were previously reported by Mears and Nash [12]. We also include data for two buildings that are discussed in detail by Wiley [13].

f-chart predictions using measured radiation and temperature data and measured loads should be compared with the measured solar contribution to meeting these loads. The f-chart procedure does not predict the weather nor the actual building loads. Comparisons have been incorrectly made between predicted solar contributions based on long-term

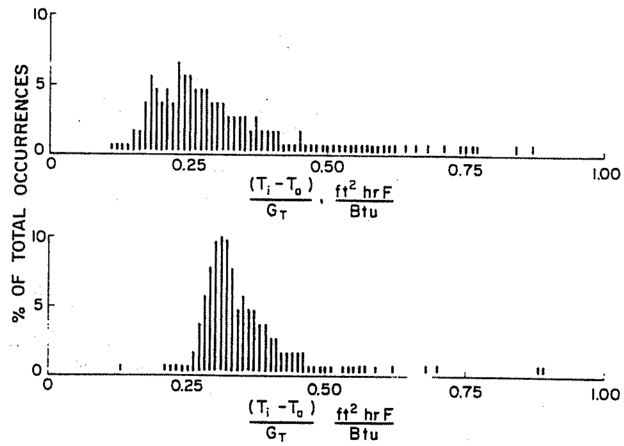

Fig. 4 Frequency of occurrence of values of $(T_i - T_a)/G_T$ for system L2 during February and July at Glendo, Wym.

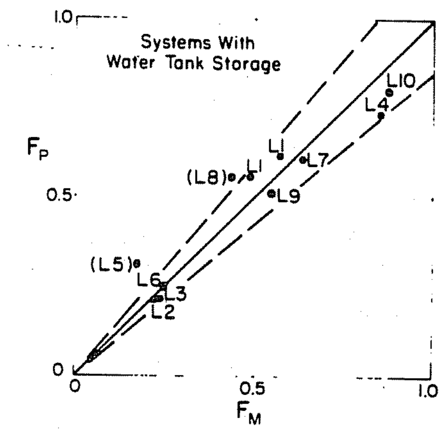

Fig. 5 Predicted compared to measured annual or seasonal performance for systems using water storage tanks

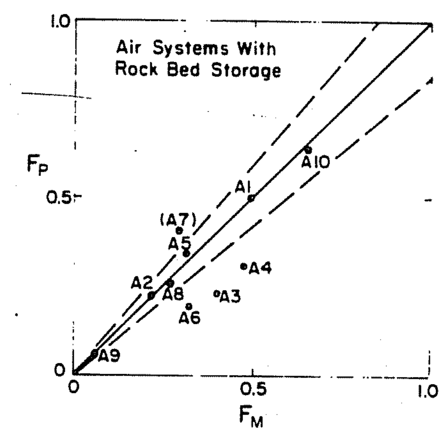

Fig. 6 Predicted compared to measured annual or seasonal performance for air systems with pebble bed storage

average meteorological data and measured solar contribution for a particular year; the year may have been very different from the long-term average.

The f-chart method requires that values of $F_R\ (\tau\alpha)$ and $F_R U_L$ be available. Laboratory measurements of these parameters, based on ASHRAE standard test procedures, are normally supplied by collector manufacturers. The *in situ* values of the parameters may, however, differ from laboratory measurements because of obvious factors such as changes in flow rate from those of the laboratory

Table 4 Characteristics and annual performance of liquid systems

System	Location	Load	A_c,m^2	Store, l	$T_{del,min}$	F_P	F_M
L2	Glendo, Wyo.	S+HW	27.3	3780	T_{room}	0.22	0.24
L3	Yosemite, Calif.	S	91	9460	32°C.	0.22	0.23
L4	Tucson, Ariz.	S+HW	179	11350	–	0.73	0.85
L5	Tunkhamock, Pa.	S+HW	19.4	450	35°C	(0.31)	(0.17)
L6	Columbia, Md.	S+HW	32.5	3780	–	0.24	0.25
L7	Ft Collins, Colo.	S+HW	50	4500	25°C	0.61	0.63
L8	Ft Collins, Colo.	S+HW	44.7	4160	25°C	(0.56)	(0.43)
L9	Medway, Mass.	S+HW	2.93	2840	21°C	0.51	0.54
L10	Blue Earth, Minn.	S	1070	75,000	–	0.79	0.86

measurements, and because of more subtle effects such as changes in loss coefficient due to interactions of buildings and collectors. The designer has the laboratory data to work with and can make corrections for flow rate, pipe and duct losses, etc. [4], while the evaluation of field installations are based on *in situ* measurements. The NSDN reports show both laboratory and *in situ* measurements of $F_R\ (\tau\alpha)_n$ and $F_R U_L$ and the values of F_P shown are based on the latter.

The NSDN reports also show another interesting fact, i.e., that collectors normally operate over limited ranges of the parameter $(T_i - T_a)/G_T$. Sample histograms of frequency of occurrence of various values of this ratio for summer and winter operation of a heating system are shown in Fig. 4. These histograms define the range over which collector tests should be done in determining $F_R U_L$ and $F_R(\tau\alpha)_n$, if there are significant nonlinearities in collector performance.

4 Predictions and Measurements

The comparisons are shown for three types of systems. These are liquid systems with energy storage in liquid tanks, air systems with storage in pebble beds, and hot water only systems. For each type of system the results are summarized on plots of F_P versus F_M. Then each specific case is discussed in enough detail to permit interpretation of the comparison. Finally, all systems comparisons are shown on a single F_P versus F_M plot. Each of the plots shows lines for ±15 percent deviation. For the NSDN systems, the referenced reports are listed in the bibliography under the same designation as is used in the tables, paragraphs and figures below.

Liquid Systems. A summary of the comparisons for liquid systems is shown in Fig. 5. The MIT House IV data of Table 3 are included for each of the two years, and are designated by L1. Other systems are also designated as L2 through L10, and the location, major characteristics, and F_P and F_M are indicated in Table 4. For each of the systems the differences between the system configuration and the *f*-chart "standard" are described and other comments on the comparison are made in paragraphs following the table. Included in this set are systems with air collectors and air to liquid heat exchangers, and systems with heat exchangers immersed in storage tanks. These systems are covered by the *f*-chart for liquid systems as long as correct values of heat exchanger effectiveness are used in calculating F_R'/F_R. The data on F_P and F_M are as reported by the authors of the sources of the information. The solar fractions in parentheses are those for which the comparison is of questionable validity.

We have checked many of the design parameters of these sytems to see if they fall in the *f*-chart range, and any discrepancies are noted. It has not been possible to check all of them, however, and flow rates through the collector are particularly uncertain.

• L2 This residential system is close to the standard *f*-chart configuration, except that drain-back freeze protection is used, the hot water exchanger is in the main storage tank, and a single hot water tank is used. Control is also close to standard.

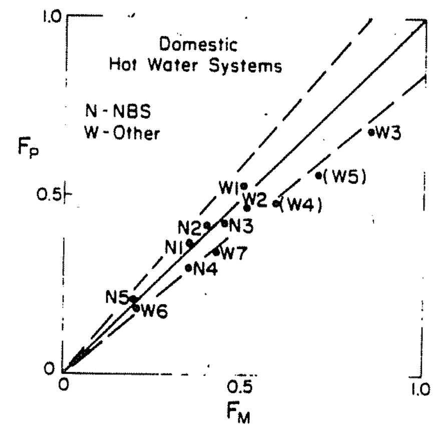

Fig. 7 Predicted compared to measured performance for domestic hot water systems

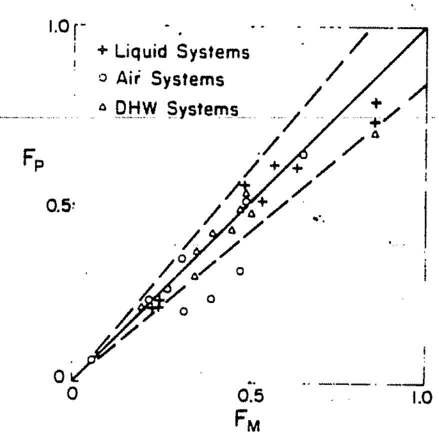

Fig. 8 Predicted compared to measured performance for all systems (excluding L5, L8, A7, W4, and W5)

• L3 The application is for a visitor's center. The system configuration is close to standard, but the collector heat exchanger is in the storage tank. The minimum temperature for heat delivery is 32°C instead of 20°C.

• L4 This residential system has two major features that differ from the standard. First, when the auxiliary heater is turned on, solar heat is not extracted from the storage tank; this would ordinarily mean that solar performance would be somewhat poorer than predicted. Second, swimming pool heating can be provided by a heat exchanger in the collector loop. During February and March solar energy was provided to the pool and was included in the loads; as the pool temperature would be lower than the main storage tank temperature during at least part of the time of collector operation, the actual performance would tend to be better than predicted. The data available do not permit satisfactory separation of these two effects, but the fact that measured performance exceeds predicted performance in this case is n

Table 5 Characteristics and annual performance of air sytems

System	Location	Load	A_c,m^2	Store, m^3	F_P	F_M
A1	Carlsbad, N.M.	S+HW	37.9	8.1	0.51	0.48
A2	Akron, Ohio	S+HW	50.7	7.64	0.22	0.24
A3	Duffield, Va.	S+HW	39.9	7.5	0.24	0.39
A4	Newman, Ga.	S+HW	36.4	9.20	0.32	0.42
A5	Huntsville, Ala.	S+HW	66.9	14.8	0.35	0.31
A6	Clinton, Miss.	S+HW	24.1	3.7	0.20	0.32
A7	Manchester, N.H.	S+HW	74.8	20.4	(0.41)	(0.29)
A8	Lincoln, Nebr.	S	44.7	9.82	0.27	0.27
A9	Canton, Ohio	S+HW	39.8	16.8	0.06	0.06
A10	Ft Collins, Colo.	S+HW	57.9	10.3	0.64	0.65

surprising. (Operation of absorption air conditioning equipment was also possible, but no cooling was done during the period of the data shown in Table 4.)

• L5 Air collectors, an air-to-water heat exchanger, and a water tank storage are used in this residential system. The house heating system is forced hot air. Direct heating of the building with solar heated air is possible. Energy storage for space heating is in two water tanks, one of which is ineffective as far as solar heating is concerned, and the capacity shown in Table 4 is for one tank only. The minimum tank temperature for energy delivery to the house is 35°C. Thus system configuration and control strategy do not match those of f-chart. The storage/collector ratio is one-half the lower limit of the range covered by f-chart. The last is probably the most important discrepancy. Also, leakage of air from the collectors may have been significant. Thus f-chart should not be used in designing or predicting the performance of this system, and the comparison of F_P and F_M is meaningless. The data are shown for the purpose of illustrating a situation where it is clear that a system falls outside of the ranges in which f-chart can be used.

• L6 The system is nearly standard, except for the configuration of the hot water subsystem, which uses a heat exchanger in the main storage tank to preheat incoming mains water when there is no water draw. The collector loop uses (evidently) drain-back freeze protection [8].

• L7 This system configuration is close to standard, and the installation is on a building serving as a CSU laboratory (House I). The collector was a Corning evacuated tubular collector, with flat absorber in the tubes; it could be represented adequately by a set of the usual collector parameters, although $F_R U_L$ was lower than most conventional collectors. T_{del} shown in the table was a minimum storage tank temperature for system turn-on in the storage-house mode; it could continue to operate at lower tank temperatures. Data are for the heating season 1977–78.

• L8 The system of L7 was rebuilt with a different type of evacuated tubular collector, an electric auxiliary source which utilized off-peak energy stored in a separate sensible heat storage unit, and other minor changes. The off-peak storage unit had relatively high thermal losses to the building; during cold weather this resulted in reduced demand for solar heat and increased use of (uncontrolled) auxiliary, and this may account for a substantial part of the difference between F_P and F_M. With significant amounts of uncontrolled auxiliary added to the building, it is questionable whether the comparison is significant. The data are for 1978–79 heating season.

• L9 This residential system is close to standard configuration. The collector heat exchanger is inside the main storage tank. The DHW system is a one-tank unit with auxiliary energy supplied to the water in the tank.

• L10 The system is for space heating only, and is a retrofit on a single-story manufacturing plant. Freeze protection is by drainback. (L9 and L10 are discussed in some detail by Kelly [13].)

Air Systems. Data are available on a larger number of air systems, and these are shown in Fig. 6 and Table 5. These systems all use pebble bed heat storage units, which are normally characterized by very effective stratification. Unknown with most air systems is the extent of leakage of air into or out of the system and its effect on system performance.

• A1 The system is on a residence, and is essentially identical to standard system except that solar heat to the building is turned off when auxiliary is turned on. Air flow rates and storage/collector ratio are very close to standard, and F_P is very nearly the same as F_M.

• A2 This system is also very close to standard, except that solar heat is not provided to the building when auxiliary is being provided to the building. This system has a heat pump auxiliary with a separate off-peak storage unit for the heat pump, but these features do not affect the solar operation.

• A3 This system is close to the standard configuration, except for two features. First, the collector-storage loop can operate while auxiliary heat is being supplied to the building; this would result in some modest performance advantage. Second, a heat pump auxiliary source is used in parallel with the solar energy system and has its own off-peak storage; this should not affect solar operation. The reason for F_M being larger than F_P is not clear.

• A4 This system is close to the standard configuration, with auxiliary energy provided by a parallel heat pump. Minimum temperatures of energy delivery to the house are 30°C air from collector or 33°C from storage. Air flow through the rock bed is horizontal, which should make little difference as long as there is no bypass of air across the top of the storage unit. The reason for F_M being larger than F_P is not clear.

• A5 The system is close to the standard configuration, with auxiliary energy provided by a parallel heat pump. Collector turn-on for collector-to-storage mode occurs when the collector temperature exceeds the temperature in the bottom of storage by 25°C and the turn-off difference is 16°C; these are higher than assumed in development of f-chart. Also, hot water consumption was very low, the preheat tank ran at higher than normal temperatures, and losses from it were probably higher than anticipated in the f-chart development. These may account for F_P being higher than F_M.

• A6 The system configuration is close to the standard. Hot water preheat is accomplished via a thermosyphon loop. Collector turn-on for collector-to-storage mode occurs when the collector outlet temperature is higher than that in the bottom of the storage unit by 22°C, and turn-off is at 15°C. The reason for F_M exceeding F_P is not clear; it may have been due in part to dust and dirt on the pyranometer which would lead to underestimated radiation on collector and reduced performance prediction.

• A7 The system configuration is close to standard, but with the rock bed horizontal. Controls and not standard. In

Table 6 **Measured and predicted values of annual solar contribution of domestic water heating systems, from NBS laboratory experiments**

System	Tank	Collector fluid	Heat exchanger	F_P	F_M
N1	1	Liquid	External	0.37	0.36
N2	2	Liquid	External	0.40	0.37
N3	1	Liquid	Internal	0.43	0.45
N4	2	Liquid	Internal	0.30	0.33
N5	1	Air	External	0.21	0.20

Table 7 **Data on water heating systems from NSDN**

System	Location	A_c, m^2	Tanks (l)	F_P	F_M
W1	Macon, Ga.	7.43	1 (454)	0.53	0.50
W2	Togus, Me.	9.75	2 (454, 151)	0.47	0.51
W3	Palm Beach Co., Fla.	7.43	1 (454)	0.69	0.85
W4	Encinitas, Calif.	6.04	2 (151, 250)	(0.49)	(0.59)
W5	Tempe, Ariz.	6.04	2 (197,197)	(0.57)	(0.71)
W6	San Diego, Calif.	48.3	2 (3790,*)	0.19	0.21
W7	Medway, Mass.	4.18	2 (302, 151)	0.35	0.43
W8	Israel	94.5	2 (4000, 2000)	0.48	0.48

the collector-to-storage mode, it is required that collector temperature be at least 8°C higher than the hot side storage temperature; this will lead to premature collector turn-off, and probably accounts for poor measured performance relative to prediction. The building was not occupied during the period of performance measurements.

• A8 The system configuration is close to standard. Collector-to-storage operation is started when collector plate temperature is 43°C and is hotter than the top of the rock bed, and continues until the plate temperature is less than 33°C (or until space heating is needed). The collector-to-space heating mode has the same requirements on plate temperature; i.e., it starts when space heating is needed and when $T_P > 43$°C, and stops when T_P drops below 33°C or heat is no longer needed.

• A9 The system is standard as far as space heating is concerned. Water heating is accomplished by a heat exchanger in an air flow loop that can be supplied with heated air from either storage or collector. F_P and F_M agree [12].

• A10 This system was on CSU House II and was evaluated during the winter of 1978–79. The system was the standard *f*-chart air system, and agreement between F_R and F_M is excellent [10].

Hot Water Systems. The third set of systems supply hot water only for residential or institutional use. The systems vary in the number of tanks used and in the method of freeze protection. Studies by Buckles and Klein [6] and others indicate that there should not be much difference among these variants, and data on all of them are included in this summary.

The National Bureau of Standards conducted a year-long careful experimental study of the laboratory performance of several hot water systems [8]. In these experiments, hot water draw was programmed to match that used in the *f*-chart development. The results of five of these experiments are shown in Table 6, which indicates the fraction of the total load (water draw plus auxiliary tank losses) supplied by solar. (The sixth system was a thermosyphon system, to which *f*-chart does not apply). These points are shown on Fig. 7, and are designated N1 to N5.

Table 7 summarizes additional data from NSDN and other sources on hot water systems. In contrast to the NBS laboratory data, these are data from field applications, and loads on the system varied widely from those assumed in developing *f*-chart. Where two tanks are used, the capacities of both of them are given in parentheses, and where only one is used, its capacity is indicated.

• W1 This residential application is a single-tank system with a jacket heat exchanger. Silicon oil is the fluid used in the collector loop. Electric resistance elements in the tank provide auxiliary. Collector turn-on occurs when the collector plate temperature exceeds the tank bottom temperature by 11°C, and turn-off occurs when this ΔT drops below 3°C. Pump flow rate is proportional to ΔT over the 11–3°C range.

• W2 This residential system is close to the standard two-tank configuration. A double-wall external collector heat exchanger is used. Pumps turn on at a temperature difference of 15°C, and off a difference of 5°C.

• W3 The system is installed on a residence, and is a single tank configuration with circulation of water through the collector. The turn-on and turn-off temperature differentials were 8°C and 2°C. Loads on the systems during much of the period of measurement were lower than expected as the building was unoccupied during part of the period. Losses from the tank of a one-tank system losses can be made up by solar. This combination of circumstances may account for the excess of F_M over F_P.

• W4 This two-tank residential system has the unique feature that solar heated water can be circulated to either of the tanks; i.e., it goes to the 151-L (40-gal) DHW tank when its temperature is less than 60°C and to the 250-L solar tank when T_{DHW} exceeds 60°C. In this arrangement, losses from the auxiliary tank can be met by solar energy, leading to improvement of performance over design. However, a combination of lighter than anticipated loads and mechanical difficulties with the system made interpretation of the results difficult. It is questionable whether *f*-chart should be used in design of this kind of system.

• W5 This system has the same two-tank configuration as system W4, and solar heated water can be pumped to either tank. This would tend to increase performance over predictions. Freeze protection is accomplished by circulating warm water through the collectors during infrequent and short periods of freezing temperatures, or by manual draining of the collector system during extended cold periods. These methods of freeze protection would tend to decrease performance relative to predictions if freezing or the threat thereof occurred very often. As with W4, it is questionable whether *f*-chart should be used to design this system. (The data shown for systems W4 and W5 tend to indicate that there is a performance advantage to be gained from piping systems so that solar heat water can go to either of two storage tanks. This is an interesting question; the data are far from conclusive.)

• W6 This system is unusual in that it includes a single large preheat tank which supplies solar preheated water to 30 separate 197-L DHW heaters, each of which supplies an apartment with hot water. However, its configuration is basically the same as that for which f-chart was developed, and agreement between F_P F_M is very good [12].

- W7 This is a standard system in all respects except for the collector heat exchanger, which is immersed in the preheat tank. The reasons for F_M exceeding F_P are not clear [12].
- W8 The system supplies hot water for an Israeli kibbutz, and is close to the standard configuration. The main difference is that the heated water from the collector heat exchanger can be shunted into the second tank if the preheat tank reaches a preassigned temperature while the collector is still operating. T_P and T_M for the year are the same [11].

It has been noted by Stoney [14] and others that many systems are operated in mild weather with auxiliary energy sources turned off. Under these circumstances, the solar fraction will be higher than a prediction based on supplying water at higher mean temperatures.

5 Summary

An overall impression of the relationships of F_P to F_M can be gained from Fig. 8, which is a composite of the data shown in Figs. 5, 6, and 7. All of the data from the other figures are included except for system L5, which is clearly not a system to be designed with f-chart, and systems L8, A7, W4, and W5, where use of f-chart is questionable.

Two general observations can be drawn from these data. First, there is a general trend of agreement between the measured and predicted seasonal performance of all three types of systems. Twenty-two of the measured values are within ± 15 percent of the predicted, while four show significantly better performance than predicted. Second, it appears from data from systems A_3, A_4, and A_6 that there might be an f-chart bias to underpredict the performance of air systems. From the information available on these systems it is not clear why these discrepancies should appear. In the authors' biased view, the difficulty in making good performance measurements may be responsible for the differences. The number of data points is too small for any one type of system to draw firm statistical conclusions.

Systems with configurations close to the standard show good agreement between predicted and measured performance, while those with significant differences do not. The collector area to storage ratio has a significant effect, as shown by the discrepancy for system L5. Finally, the control temperatures do not have a major effect on performance air systems, based on data for systems A4–A8. The set temperatures for these systems all differ from those for the standard. The same comments cannot be made for liquid systems, and considerably more information is needed (including more very careful measurements on air systems) before clear conclusions can be reached.

Mears and Nash [12] stated in their conclusion that the modified f-chart analysis technique "yields good agreement between estimated and measured system performance for properly operating solar hot water and/or space heating systems..." The additional data shown in this paper bear out their conclusion. It is also clear that f-chart must only be used for systems for which it is designed, and within the specified ranges of design parameters, such as storage capacity and air flow rates.

References[1]

1 Klein, S. A., Beckman, W. A., and Duffie, J. A., "A Design Procedure for Solar Heating Systems," *Solar Energy*, Vol. 18, 1976, p. 113.

2 Klein, S. A., Beckman, W. A., and Duffie, J. A., "A Design Procedure for Solar Air Heating Systems," *Solar Energy*, Vol. 19, 1977, p. 509.

3 Beckman, W. A., Klein, S. A., and Duffie, J. A., *Solar Heating Design*, Wiley-Interscience, New York, 1977.

4 Duffie, J. A., and Beckman, W. A., *Solar Engineering of Thermal Processes*, Wiley-Interscience, New York, 1980.

5 Beckman, W. A., "Duct and Pipe Losses in Solar Energy Systems," *Solar Energy*, Vol. 21, 1978, p. 531.

6 Buckles, W. E., and Klein, S. A., "Analysis of Solar Domestic Hot Water Heaters," *Solar Energy*, Vol. 25, 1980, p. 417.

7 Engebretson, C. D., "The Use of Solar Energy for Space Heating—MIT House IV," *Proceedings of the U.N. Conference of New Sources of Energy*, Vol. 5, p. 159.

8 Fanney, A. H., personal communication on the NBS Solar Domestic Hot Water Test Facility.

9 Duff, W. S., and Lof, G.O.G., "The Performance of Evacuated Tubular Solar Collectors in a Residential Heating and Cooling System," Report COO-2577-20 by Colorado State University to DOE, Mar. 1981.

10 Karaki, S., Brisbane, T. E., Waterbury, S. S., and Lantz, T. G., "Performance Evaluation of a State-of-the-Art Solar Air-Heating System With Auxiliary Heat Pump," Report COO/30122-4 by Colorado State University to DOE, Jan. 1980.

11 Faiman, D., Feuermann, D., Gordon, J. M., and Govaer, D., "F-Chart, Theory Versus Reality: An Israel Case Study," paper communicated to authors, 1981.

12 Mears, J. C., and Nash, J. M., "Performance Evaluation of Solar Energy Systems Using a Modified f-Chart Analysis," ASME Paper No. 80-C2/Sol 22.

13 Kelly, C. J., "Comparison of Field Measured Performance with F-Chart 3.0 and F-Chart 4.0 Predictions," *Solar Engineering—1982*, ASME, New York.

14 Stoney, W. E., personal communication.

[1] The following are DOE/NASA Contractor Report numbers for reports on the NSDN systems. All reports were prepared by the IBM Corporation.

L2	DOE/NASA CR-161520	A3	DOE/NASA CR-161507	W1	DOE/NASA CR-161380
L3	DOE/NASA CR-161539	A4	DOE/NASA CR-161494	W2	DOE/NASA CR-161383
L4	DOE/NASA CR-161450	A5	DOE/NASA CR-161464	W3	DOE/NASA CR-161379
L5	DOE/NASA CR-161392	A6	DOE/NASA CR-161509	W4	DOE/NASA CR-161481
A1	DOE/NASA CR-161508	A7	DOE/NASA CR-161471	W5	DOE/NASA CR-161466
A2	DOE/NASA CR-161465	A8	DOE/NASA CR-161495		